Pergamon

Int. J. Solids Structures Vol. 33, No. 6, pp. 795-810, 1996

0020-7683/96 $9.50 + .00

0020-7683(95)00075-5

NOTES ON THE BEHAVIOR OF TRANSVERSELY LOADED INEXTENSIBLE PLATES

PAVEL ŠIMÁČEK

Center for Composite Materials, Department of Mechanical Engineering, University of Delaware, Newark, DE 19716, U.S.A.

and

VICTOR N. KALIAKIN†

Department of Civil Engineering, University of Delaware, Newark, DE 19716, U.S.A.

(Received 21 October 1994; in revised form 14 March 1995)

Abstract — The governing equations for incompressible plates exhibiting a direction of inextensibility are developed in this paper. The motivation for the analysis of such materials is the rise in popularity of fiber-reinforced thermoplastic composites, though the conclusions reached apply equally well to incompressible materials exhibiting very large degrees of anisotropy. In the course of the development, the importance of transverse shear response is demonstrated, indicating that lower order plate theories cannot be used to realistically model incompressible inextensible materials. As is the case with other plate theories, the in-plane and transverse responses uncouple. A sample analysis, involving only the transverse response, is performed and the results are compared to a simplified solution that is likewise derived herein.

INTRODUCTION

While most researchers in solid and fluid mechanics are familiar with the constraint of incompressibility, the consequences of constraining the extensional deformation in one or more directions are not widely understood. Recent developments in the area of composite materials and, to a lesser degree, in the study of crystalline microstructure (Coffin, 1993a), have necessitated consideration of the latter constraint.

In the area of composites, inextensibility is realized when a thermoplastic matrix is reinforced by large volume fractions of fibers. One advantage of such a material is that the matrix can be melted, and the original body shaped into a more complex part. Of particular interest to the present development is the process of "sheet forming". During this process, relatively thin sheets of pre-prepared material are melted and formed into three-dimensional parts; this process closely resembles the forming of metal or unreinforced thermoplastic sheets. Assuming a suitable idealization is used for the viscous and nearly incompressible matrix, the behavior of the composite is then dictated by the nature of the reinforcement.

Consider first the case of reinforcement consisting of continuous fibers. During melting of the matrix the fibers remain solid. Assuming negligible elastic deformations, it follows that the fibers cannot extend. Furthermore, due to the extremely small fiber diameters, the elastic bending stiffness of the reinforcement is negligible. Thus, continuous fibers are assumed to be perfectly inextensible and ideally flexible. As a result, the composite material possesses a direction of inextensibility parallel to the fibers.

If the fibers are long but discontinuous, the material remains extensible in all directions. However, if high volume fractions of long, well-aligned fibers are used (a desirable practice, owing to the properties of the finished product), the ratio of material parameters (e.g. viscosities or moduli) in the longitudinal (fiber) direction to those in the transverse directions may exceed 10^5 (Pipes *et al.*, 1994). Thus, although strictly speaking it is only approximately inextensible, for all practical purposes this "hyperanisotropic" material behaves as an inextensible medium. A parallel phenomenon exists with the constraint of incompressibility.

†Author to whom correspondence should be addressed.

Namely, nearly incompressible media behave essentially in the same manner as fully incompressible media.

Interest in fiber-reinforced thermoplastic composites has led to several efforts to quantify their behavior. Such materials have been shown to correspond to Spencer's class of "ideal fiber-reinforced materials" (Spencer, 1984). The existence and regularity of solutions for fiber-reinforced thermoplastic composites has been studied by Rogers (1984). A number of solutions for such materials have also been developed (Rogers and Pipkin, 1971; Rogers, 1984). However, since they assume a state of plane strain, these solutions are not directly applicable to the simulation of forming processes involving thin sheets. More applicable to such processes are the analytical (Coffin, 1993b; Šimáček, 1994) and numerical (Beaussart, 1990; Ó Brádaigh, 1990; Ó Brádaigh and Pipes, 1992; Šimáček, 1994; Šimáček *et al.*, 1993) solutions performed assuming a plane stress idealization.

Still, most actual forming processes involve the transverse loading of thin, and initially flat, sheets. As such, any realistic simulation of this process must be three-dimensional in nature. Perhaps the simplest approach, which does not always possess sufficient accuracy, idealizes the fiber-reinforced thermoplastic composite as a membrane (Šimáček, 1994). However, if infinitesimal displacements and displacement gradients are assumed, this idealization cannot possibly work for a transversely loaded flat sheet. Of course, one remedy is to assume finite displacements. A second, and practically more realistic, approach is to develop a solution for incompressible plates possessing a direction of inextensibility. The development of such a solution constitutes the subject of this paper.

Besides being a rather interesting undertaking, a solution for incompressible and inextensible plates is desirable for several reasons. First, the solution may give insight into the most important load transfer mechanisms for plates possessing the aforementioned kinematic constraints. Second, since upon transverse loading actual composite sheets may no longer remain flat, and since a membrane formulation can be used to compute subsequent deformations, the plate solution could be used to initiate this formulation. Finally, should the membrane approach fail to give accurate solutions, the plate formulation may provide a reasonable basis for the development of a thick shell formulation.

THE INEXTENSIBILITY CONSTRAINT AND ITS IMPLICATIONS

A plate possessing a direction of inextensibility in its plane exhibits behavior different from that of an ordinary extensible plate. To better illustrate this fact, albeit in a rather heuristic manner, consider the simpler case of a beam (Fig. 1). Depending upon the level of anisotropy, an ordinary (extensible) material behaves more or less in accordance with

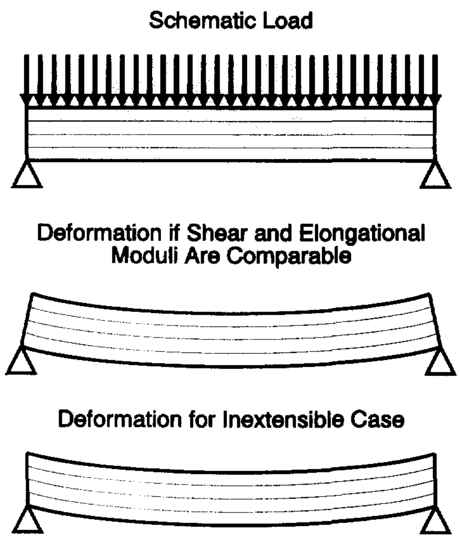

Fig. 1. Shear deformation for inextensible beam subjected to transverse load.

the kinematic assumptions of Bernoulli. If, on the other hand, the inextensibility constraint prevents longitudinal elongation, then any transverse loading is carried by both shearing and bending, with only the former contributing to the deflection. This observation holds regardless of the depth of the beam.

Now the above discussion was simplified by the essentially one-dimensional nature of the problem. In the case of a plate, the material can also bend in a direction perpendicular to the direction of inextensibility; the behavior in the direction of inextensibility should mimic the behavior of the beam depicted in Fig. 1. A pertinent question to be asked at this point is which deformation mode is dominant. Although other factors come into play, it is safe to expect longitudinal shearing to be an important deformation mode.

DERIVATION OF GOVERNING EQUATIONS

Simplifying assumptions

Guided by the observations of the previous section, some simplifying assumptions must be made prior to derivation of the governing plate equations. First, although the actual fiber-reinforced material is non-homogeneous, we will assume that it behaves like a transversely isotropic Newtonian fluid with a single family of inextensible reinforcing fibers (Beaussart, 1990). The axis of material symmetry is taken coincident with the fiber direction. In any reasonable analysis of actual structures made of composite materials, such an assumption is typically utilized.

Secondly, we assume that throughout the continuum, the axis of material symmetry (i.e. the inextensibility direction) remains unchanged. The associated coordinate system, located at the middle surface of the plate, is depicted in Fig. 2. Although such an assumption is acceptable for the case of fiber-reinforced plates, it must be relaxed if generalized forming conditions are simulated. This is because during an actual forming process the reinforcing fibers typically do not remain parallel, though their direction forms a fairly smooth vector field.

Thirdly, due to the low rates associated with the forming of fiber-reinforced thermoplastic composites, conditions of Stokes flow (with negligible inertia effects) are assumed. In light of this and the first assumption, the continuum is thus assumed to be perfectly incompressible as well as perfectly inextensible in the fiber direction. While this is obviously an idealization, it appears to be reasonably close to reality in actual forming processes involving such materials (Ó Brádaigh, 1990).

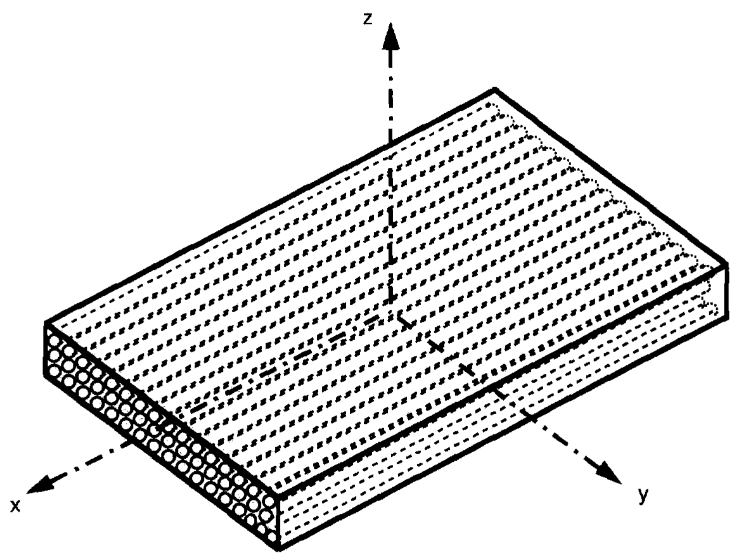

Fig. 2. Geometry and coordinate system for fiber-reinforced plate problem of interest.

In light of the above assumptions, the constitutive relations for a transversely isotropic Newtonian fluid can thus be written in the form presented by Ó Brádaigh (1990), who follows Spencer (1984):

$$\begin{Bmatrix} \sigma_{xx} \\ \sigma_{yy} \\ \sigma_{zz} \\ \sigma_{yz} \\ \sigma_{xz} \\ \sigma_{xy} \end{Bmatrix} = \begin{bmatrix} 2(2\eta_L-\eta_T) & 0 & 0 & 0 & 0 & 0 \\ 0 & 2\eta_T & 0 & 0 & 0 & 0 \\ 0 & 0 & 2\eta_T & 0 & 0 & 0 \\ 0 & 0 & 0 & 2\eta_L & 0 & 0 \\ 0 & 0 & 0 & 0 & 2\eta_L & 0 \\ 0 & 0 & 0 & 0 & 0 & 2\eta_L \end{bmatrix} \begin{Bmatrix} d_{xx} \\ d_{yy} \\ d_{zz} \\ d_{yz} \\ d_{xz} \\ d_{xy} \end{Bmatrix} - \begin{Bmatrix} T-p \\ -p \\ -p \\ 0 \\ 0 \\ 0 \end{Bmatrix}. \quad (1)$$

In eqn (1), σ_{xx}, σ_{yy}, etc. denote stresses and d_{xx}, d_{yy}, etc. denote strain rates. The quantities η_L and η_T denote, respectively, the longitudinal and transverse shear viscosities. Finally, the constraint variables T and p denote the fiber tension stress and pressure, respectively. At this point in the development it is important to note the formal analogy between the above constitutive relations and those associated with ideal, transversely isotropic elastic solids (Spencer, 1984). More precisely, in the analysis of such solids, displacements replace velocities, σ_{xx}, σ_{yy}, etc. again denote stresses, d_{xx}, d_{yy}, etc. now denote strains, η_L and η_T denote, respectively, the longitudinal and transverse shear moduli, and T and p again denote the fiber tension stress and pressure, respectively. This analogy will prove useful in the subsequent derivation of the governing equations.

The next assumptions are kinematic in nature. Namely, infinitesimal displacements and displacement gradients are assumed. Finally, for a thin plate with the coordinate system depicted in Fig. 2, we assume the following velocity field:

$$u_x(x,y) = u(x,y) + z\alpha(x,y) \quad (2a)$$

$$u_y(x,y) = v(x,y) + z\beta(x,y) \quad (2b)$$

$$u_z(x,y) = w(x,y) + z\gamma_1(x,y) + z^2\gamma_2(x,y). \quad (2c)$$

In eqns (2a–c) u_x, u_y and u_z denote velocity components in the coordinate directions, and u, v and w represent the velocity components of the middle surface in the x-, y- and z-coordinate directions, respectively. The quantities α and β denote fiber rotations about the y- and x-axes, respectively. The functional form for u_z appearing in eqn (2c) was chosen to allow not only for variations in the deformation through the thickness, but also for the incompressibility constraint to be correctly accounted for in the governing equations. The above velocity field corresponds to the Reissner–Mindlin assumptions for displacements in a plate.

Having assumed a velocity field, the following stress resultants are introduced:

$$P_1(x,y) \equiv \int_{-h/2}^{h/2} p\,\mathrm{d}z \quad (3a)$$

$$P_2(x,y) \equiv \int_{-h/2}^{h/2} pz\,\mathrm{d}z \quad (3b)$$

$$T_1(x,y) \equiv \int_{-h/2}^{h/2} T\,\mathrm{d}z \quad (3c)$$

$$T_2(x, y) \equiv \int_{-h/2}^{h/2} Tz\,\mathrm{d}z. \tag{3d}$$

Development of the functional

The governing partial differential equations and associated boundary conditions will be derived using a variational approach. Since no convenient functional exists for the case of Stokes flow, we make use of the aforementioned analogy to the transversely isotropic elastic continuum. As such, the basis for the functional is the total potential. The functional must be modified in order to account for the kinematic constraints of inextensibility

$$d_{xx} = 0 \tag{4}$$

and incompressibility

$$d_{xx} + d_{yy} + d_{zz} = 0. \tag{5}$$

Associating the Lagrange multipliers T and p with the above constraints, we obtain the final form of the functional:

$$\Pi = \frac{1}{2}\int_V [2(2\eta_L - \eta_T)(d_{xx})^2 + 2\eta_T(d_{yy})^2 + 2\eta_T(d_{zz})^2 + \eta_T(2d_{yz})^2 + \eta_L(2d_{xz})^2 + \eta_L(2d_{xy})^2]\,\mathrm{d}V + \int_V Td_{xx}\,\mathrm{d}V - \int_V p(d_{xx} + d_{yy} + d_{zz})\,\mathrm{d}V - \int_V (b_x u_x + b_y u_y + b_z u_z)\,\mathrm{d}V - \int_\Gamma (t_x u_x + t_y u_y + t_z u_z)\,\mathrm{d}\Gamma, \tag{6}$$

where the quantities b_x, b_y and b_z denote body force components acting over the body of volume V, and t_x, t_y and t_z represent components of the surface traction acting over some portion of the body's surface Γ. Finally, engineering measures of shear strain have been used. Before proceeding, the body force components are assumed to be negligible. This simplification is justified by the relatively thin plates under consideration. Furthermore, the surface traction is specialized in the following manner:

$$\mathbf{t} = \{t_x^- \; t_y^- \; t_z^-\}^T \quad \text{at } z = -h/2 \tag{7a}$$

$$\mathbf{t} = \{t_x^+ \; t_y^+ \; t_z^+\}^T \quad \text{at } z = h/2, \tag{7b}$$

where the superscript T denotes the operation of matrix transposition.

Equations (2) are next substituted into the infinitesimal strain–displacement relations. The resulting expressions, along with the quantities defined in eqns (3), are then introduced into eqn (6). Finally, the resulting functional is minimized with respect to the unknowns u, v, w, α, β, γ_1, γ_2, P_1, P_2, T_1 and T_2. As a result, we obtain the following equations:

$$\frac{\partial u}{\partial x} = 0 \tag{8}$$

$$\frac{\partial \alpha}{\partial x} = 0, \tag{9}$$

which express the constraint of inextensibility, and

$$\frac{\partial u}{\partial x}+\frac{\partial v}{\partial y}+\gamma_1=0 \tag{10}$$

$$\frac{\partial \alpha}{\partial x}+\frac{\partial \beta}{\partial y}+2\gamma_2=0, \tag{11}$$

which express the incompressibility constraint. Next, we obtain the equilibrium equations associated with the three coordinate directions, namely

$$2h(2\eta_{\mathrm{L}}-\eta_{\mathrm{T}})\frac{\partial^2 u}{\partial x^2}+2h\eta_{\mathrm{L}}\left(\frac{\partial^2 u}{\partial y^2}+\frac{\partial^2 v}{\partial x\,\partial y}\right)+\frac{\partial T_1}{\partial x}-\frac{\partial P_1}{\partial x}+(t_x^-+t_x^+)=0 \tag{12}$$

$$2h\eta_{\mathrm{T}}\frac{\partial^2 v}{\partial y^2}+2h\eta_{\mathrm{L}}\left(\frac{\partial^2 u}{\partial x\,\partial y}+\frac{\partial^2 v}{\partial x^2}\right)-\frac{\partial P_1}{\partial y}+(t_y^-+t_y^+)=0 \tag{13}$$

$$2h\eta_{\mathrm{L}}\left(\frac{\partial^2 w}{\partial x^2}+\frac{\partial^2 w}{\partial y^2}+\frac{\partial \alpha}{\partial x}+\frac{\partial \beta}{\partial y}\right)+\frac{h^3\eta_{\mathrm{L}}}{6}\left(\frac{\partial^2 \gamma_2}{\partial x^2}+\frac{\partial^2 \gamma_2}{\partial y^2}\right)+(t_z^-+t_z^+)=0. \tag{14}$$

The equilibrium equations associated with functional minimization with respect to α and β are given by the expressions

$$\frac{h^3}{6}(2\eta_{\mathrm{L}}-\eta_{\mathrm{T}})\frac{\partial^2 \alpha}{\partial x^2}+\frac{h^3}{6}\eta_{\mathrm{L}}\left(\frac{\partial^2 \alpha}{\partial y^2}+\frac{\partial^2 \beta}{\partial x\,\partial y}-\frac{\partial \gamma_2}{\partial x}\right)-2h\eta_{\mathrm{L}}\left(\alpha+\frac{\partial w}{\partial x}\right)$$
$$+\frac{\partial T_2}{\partial x}-\frac{\partial P_2}{\partial x}-\frac{h}{2}(t_x^--t_x^+)=0 \tag{15}$$

$$\frac{h^3}{6}\eta_{\mathrm{T}}\frac{\partial^2 \beta}{\partial y^2}+\frac{h^3}{6}\eta_{\mathrm{L}}\left(\frac{\partial^2 \alpha}{\partial x\,\partial y}+\frac{\partial^2 \beta}{\partial x^2}-\frac{\partial \gamma_2}{\partial y}\right)-2h\eta_{\mathrm{L}}\left(\beta+\frac{\partial w}{\partial y}\right)-\frac{\partial P_2}{\partial y}-\frac{h}{2}(t_y^--t_y^+)=0, \tag{16}$$

which represent the balance of angular momentum.

Finally, there are two additional equations associated with the weighted equilibrium in the z-direction:

$$2h\eta_{\mathrm{T}}\gamma_1-\frac{h^3}{6}\eta_{\mathrm{L}}\left(\frac{\partial^2 \gamma_1}{\partial x^2}+\frac{\partial^2 \gamma_1}{\partial y^2}\right)-P_1+\frac{h}{2}(t_z^--t_z^+)=0 \tag{17}$$

$$\frac{2h^3}{3}\eta_{\mathrm{T}}\gamma_2-\frac{h^3}{6}\eta_{\mathrm{L}}\left(\frac{\partial^2 w}{\partial x^2}+\frac{\partial^2 w}{\partial y^2}+\frac{\partial \alpha}{\partial x}+\frac{\partial \beta}{\partial y}\right)-\frac{h^5\eta_{\mathrm{L}}}{40}\left(\frac{\partial^2 \gamma_2}{\partial x^2}+\frac{\partial^2 \gamma_2}{\partial y^2}\right)$$
$$-2P_2-\frac{h^2}{4}(t_z^-+t_z^+)=0. \tag{18}$$

Equations (8)–(18) thus constitute 11 governing differential equations in the unknowns u, v, w, α, β, γ_1, γ_2, P_1, P_2, T_1 and T_2. Minimization of the functional also yields seven boundary conditions (minimization with respect to P_1, P_2, T_1 and T_2 produces no boundary conditions). The first three of these involve prescribed translations or linear tractions along the boundary:

u or f_u prescribed, where

$$f_u = \left[2h(2\eta_L - \eta_T)\frac{\partial u}{\partial x} + T_1 - P_1\right]n_x + 2h\eta_L\left[\frac{\partial u}{\partial y} + \frac{\partial v}{\partial x}\right]n_y \tag{19}$$

v or f_v prescribed, where

$$f_v = 2h\eta_L\left[\frac{\partial u}{\partial y} + \frac{\partial v}{\partial x}\right]n_x + \left[2h\eta_T\frac{\partial v}{\partial y} - P_1\right]n_y \tag{20}$$

w or f_w prescribed, where

$$f_w = 2h\eta_L\left[\alpha + \frac{\partial w}{\partial x} + \frac{h^2}{12}\frac{\partial \gamma_2}{\partial x}\right]n_x + 2h\eta_L\left[\beta + \frac{\partial w}{\partial y} + \frac{h^2}{12}\frac{\partial \gamma_2}{\partial y}\right]n_y. \tag{21}$$

The quantities n_x and n_y appearing in eqns (19)–(21) represent components of the outward unit normal in the x- and y-directions, respectively. The next two boundary conditions involve prescribed rotations or moments per unit length along the boundary:

α or f_α prescribed, where

$$f_\alpha = \left[\frac{h^3}{6}(2\eta_L - \eta_T)\frac{\partial \alpha}{\partial x} + T_2 - P_2\right]n_x + \frac{h^3}{6}\eta_L\left[\frac{\partial \alpha}{\partial y} + \frac{\partial \beta}{\partial x}\right]n_y \tag{22}$$

β or f_β prescribed, where

$$f_\beta = \frac{h^3}{6}\eta_L\left[\frac{\partial \alpha}{\partial y} + \frac{\partial \beta}{\partial x}\right]n_x + \left[\frac{h^3}{6}\eta_T\frac{\partial \beta}{\partial y} - P_2\right]n_y. \tag{23}$$

The final two boundary conditions are associated with the distribution of the shear stress along the boundary:

γ_1 or f_{γ_1} prescribed, where

$$f_{\gamma_1} = \frac{h^3}{6}\eta_L\left[\frac{\partial \gamma_1}{\partial x}n_x + \frac{\partial \gamma_1}{\partial y}n_y\right] \tag{24}$$

γ_2 or f_{γ_2} prescribed, where

$$f_{\gamma_2} = h^3\eta_L\left[\frac{1}{6}\left(\alpha + \frac{\partial w}{\partial x}\right) + \frac{h^2}{40}\frac{\partial \gamma_2}{\partial x}\right]n_x + h^3\eta_L\left[\frac{1}{6}\left(\beta + \frac{\partial w}{\partial y}\right) + \frac{h^2}{40}\frac{\partial \gamma_2}{\partial y}\right]n_y. \tag{25}$$

The boundary conditions given in eqns (24) and (25) are somewhat unfamiliar and perhaps a bit non-intuitive. However, as will be shown subsequently, the latter one, which is applicable only to the transverse response, does not significantly affect the solution.

At this point, the formulation appears to be quite complex. However, as with most ordinary plate solutions, a fundamental simplification is available. Namely, both the governing equations and the boundary conditions can readily be separated into the following two groups:

Equations (8), (10), (12), (13) and (17), together with the boundary conditions of eqns (19), (20) and (24), describe the in-plane deformation. This system of equations is independent of the remaining ones; solution of the system yields values for u, v, γ_1, T_1 and P_1.

Equations (9), (11), (14)–(16) and (18), together with the boundary conditions of eqns (21)–(23) and (25), describe the transverse deformation. Solution of this system of equations yields values for w, α, β, γ_2, T_2 and P_2.

Since the transverse behavior of an incompressible plate exhibiting a direction of inextensibility is of particular interest to the present development, we shall concentrate on the second group of equations and boundary conditions. It is worth noting in passing that due to the presence of the pressure resultant P_1 and non-zero transverse deformation, this problem is not the same as the one solved by Rogers (1984), who assumed a plane strain idealization. Neither is it the same as the problem solved by Beaussart (1990), Ó Brádaigh (1990) or Šimáček (1994), who assumed conditions of plane stress, and thus no presence of P_1 or γ_1.

STUDY OF TRANSVERSE BEHAVIOR

To facilitate the study of the transverse behavior, we assume a simplified loading involving no shearing tractions on either surface and no normal traction on the surface $z = h/2$. The only non-zero load is a pressure $t_z^- = q$ acting normal to the surface $z = -h/2$ in the positive direction. In light of this simplified loading system, eqns (9), (11), (14)–(16) and (18) reduce to

$$\frac{\partial \alpha}{\partial x} = 0 \tag{26}$$

$$\frac{\partial \alpha}{\partial x} + \frac{\partial \beta}{\partial y} + 2\gamma_2 = 0 \tag{27}$$

$$2h\eta_L\left(\nabla^2 w_0 + \frac{\partial \alpha}{\partial x} + \frac{\partial \beta}{\partial y}\right) + \frac{h^3\eta_L}{6}(\nabla^2\gamma_2) + q = 0 \tag{28}$$

$$\frac{h^3}{6}(2\eta_L - \eta_T)\frac{\partial^2 \alpha}{\partial x^2} + \frac{h^3}{6}\eta_L\left(\frac{\partial^2 \alpha}{\partial y^2} + \frac{\partial^2 \beta}{\partial x \partial y} - \frac{\partial \gamma_2}{\partial x}\right) - 2h\eta_L\left(\alpha + \frac{\partial w}{\partial x}\right) + \frac{\partial T_2}{\partial x} - \frac{\partial P_2}{\partial x} = 0 \tag{29}$$

$$\frac{h^3}{6}\eta_T\frac{\partial^2 \beta}{\partial y^2} + \frac{h^3}{6}\eta_L\left(\frac{\partial^2 \alpha}{\partial x \partial y} + \frac{\partial^2 \beta}{\partial x^2} - \frac{\partial \gamma_2}{\partial y}\right) - 2h\eta_L\left(\beta + \frac{\partial w}{\partial y}\right) - \frac{\partial P_2}{\partial y} = 0 \tag{30}$$

$$\frac{2h^3}{3}\eta_T\gamma_2 - \frac{h^3}{6}\eta_L\left(\nabla^2 w + \frac{\partial \alpha}{\partial x} + \frac{\partial \beta}{\partial y}\right) - \frac{h^5\eta_L}{40}(\nabla^2\gamma_2) - 2P_2 - \frac{h^2}{4}q = 0. \tag{31}$$

The above system of six equations is thus solved for the unknowns w, α, β, γ_2, P_2 and T_2. To simplify the system, we use eqn (26) to eliminate all derivatives of α with respect to x in the remaining equations. Furthermore, assuming sufficient smoothness, from eqn (27) it follows that

$$\gamma_2 = -\frac{1}{2}\frac{\partial \beta}{\partial y}. \tag{32}$$

Substitution of this expression into eqns (28)–(31) reduces them to

$$2h\eta_L\left(\nabla^2 w+\frac{\partial\beta}{\partial y}\right)-\frac{h^3\eta_L}{12}\frac{\partial(\nabla^2\beta)}{\partial y}+q=0 \tag{33}$$

$$\frac{h^3}{6}\eta_L\left(\frac{\partial^2\alpha}{\partial y^2}+\frac{\partial^2\beta}{\partial x\partial y}+\frac{1}{2}\frac{\partial^2\beta}{\partial x\partial y}\right)-2h\eta_L\left(\alpha+\frac{\partial w}{\partial x}\right)+\frac{\partial T_2}{\partial x}-\frac{\partial P_2}{\partial x}=0 \tag{34}$$

$$\frac{h^3}{6}\eta_T\frac{\partial^2\beta}{\partial y^2}+\frac{h^3}{6}\eta_L\left(\frac{\partial^2\beta}{\partial x^2}+\frac{1}{2}\frac{\partial^2\beta}{\partial y^2}\right)-2h\eta_L\left(\beta+\frac{\partial w}{\partial y}\right)-\frac{\partial P_2}{\partial y}=0 \tag{35}$$

$$-\frac{h^3}{3}\eta_T\frac{\partial\beta}{\partial y}-\frac{h^3}{6}\eta_L\left(\nabla^2 w+\frac{\partial\beta}{\partial y}\right)+\frac{h^5\eta_L}{80}\frac{\partial(\nabla^2\beta)}{\partial y}-2P_2-\frac{h^2}{4}q=0. \tag{36}$$

Although α is still present in eqn (34), it is just a function of y that will be determined from the boundary conditions. Also, since we are not overly interested in the value of T_2, and since it appears only in eqn (34), we need not consider this equation further. Solving eqn (36) for P_2 gives

$$P_2=-\frac{h^3}{6}\eta_T\frac{\partial\beta}{\partial y}-\frac{h^3}{12}\eta_L\left(\nabla^2 w+\frac{\partial\beta}{\partial y}\right)+\frac{h^5\eta_L}{160}\frac{\partial(\nabla^2\beta)}{\partial y}-\frac{h^2}{8}q. \tag{37}$$

Differentiating eqn (37) with respect to y and substituting the resulting expression into eqn (35) gives

$$\frac{h^3}{3}\eta_T\frac{\partial^2\beta}{\partial y^2}-\frac{h^5}{160}\eta_L\frac{\partial^2(\nabla^2\beta)}{\partial y^2}+\frac{h^3}{6}\eta_L\left(\nabla^2\beta+\frac{1}{2}\frac{\partial(\nabla^2 w)}{\partial y}\right)-2h\eta_L\left(\beta+\frac{\partial w}{\partial y}\right)+\frac{h^2}{8}\frac{\partial q}{\partial y}=0. \tag{38}$$

Equations (38) and (33) now contain only the two unknowns w and β. A reasonable simplification of the original problem has thus been realized.

In order to properly pose such a problem, we need to examine the boundary conditions available. In light of eqn (26), and using eqn (32), the boundary conditions given in eqns (21)–(23) and (25) simplify. Furthermore, where possible γ_2 and P_2 should be eliminated in favor of β and w.

We begin with the boundary condition involving a specified value of the transverse displacement w of the middle surface (the more common case), or a transverse shear traction f_w specified along the boundary. The latter, originally defined in eqn (21), now simplifies to

$$f_w=2h\eta_L\left[\alpha+\frac{\partial w}{\partial x}-\frac{h^2}{24}\frac{\partial^2\beta}{\partial x\partial y}\right]n_x+2h\eta_L\left[\beta+\frac{\partial w}{\partial y}-\frac{h^2}{24}\frac{\partial^2\beta}{\partial y^2}\right]n_y. \tag{39}$$

The next two boundary conditions describe prescribed rotations or bending moments applied along the boundary [see eqns (22) and (23)], i.e.

α or f_α prescribed, where

$$f_\alpha=[T_2-P_2]n_x+\frac{h^3}{6}\eta_L\left[\frac{\partial\alpha}{\partial y}+\frac{\partial\beta}{\partial x}\right]n_y \tag{40}$$

β or f_β prescribed, where

$$f_\beta=\frac{h^3}{6}\eta_L\left[\frac{\partial\alpha}{\partial y}+\frac{\partial\beta}{\partial x}\right]n_x+\left[\frac{h^3}{6}\eta_T\frac{\partial\beta}{\partial y}-P_2\right]n_y. \tag{41}$$

Note that although eqn (40) involves α and T_2, it might be superfluous so long as we are dealing with β and w only. However, if moment is prescribed in eqn (41), knowledge of α is essential for this boundary condition as well. Moreover, P_2, which is substituted into eqns (40) and (41) from eqn (37), introduces third derivatives of β and second derivatives of w. It is thus much simpler to deal with displacement boundary conditions than with prescribed tractions.

Two details concerning eqns (40) and (41) are noteworthy. First, we know from eqn (26) that $\alpha = \alpha(y)$ only. Thus, if the value of α is prescribed at two points with equal y-coordinates, it has to be the same at those two points. Second, T_2 will be non-unique much in the same way as that described for plane strain by Rogers (1984) and for plane stress by Šimáček *et al.* (1993), and by Šimáček (1994). This non-uniqueness can complicate numerical solution of the problem.

The final boundary condition utilized is

$$\gamma_2 = \left(-\frac{\partial\beta}{\partial y}\right) \text{or} f_{\gamma_2} \text{ prescribed, where}$$

$$f_{\gamma_2} = h^3\eta_L\left[\frac{1}{6}\left(\alpha+\frac{\partial w}{\partial x}\right)-\frac{h^2}{80}\frac{\partial^2\beta}{\partial x\,\partial y}\right]n_x + h^3\eta_L\left[\frac{1}{6}\left(\beta+\frac{\partial w}{\partial y}\right)-\frac{h^2}{80}\frac{\partial^2\beta}{\partial y^2}\right]n_y. \quad (42)$$

This condition is associated with the incompressibility constraint and deals with the distribution of either the transverse contraction or the normal transverse shear traction on the boundary. We can likewise express f_{γ_2} as

$$f_{\gamma_2} = \int_{-h/2}^{h/2} (\sigma_{xz}n_x + \sigma_{yz}n_y)z^2\,dz. \quad (43)$$

As shown in Fig. 3, this boundary condition has at least two simple distinct cases. If the end is ideally fixed (type I), no transverse contraction is possible and thus $\gamma_2 = -\partial\beta/\partial y = 0$. On the other hand, if the end is free, the transverse shear traction is zero. Although boundary conditions involving γ_2 are somewhat non-intuitive, as will be shown in a subsequent example, they fortunately do not significantly affect the solution.

Before proceeding to an example involving the solution of the governing equations, we desire to gain further insight into eqns (33) and (38). As such, assuming sufficient smoothness of the unknowns, suppose that the in-plane dimensions of the plate are of order

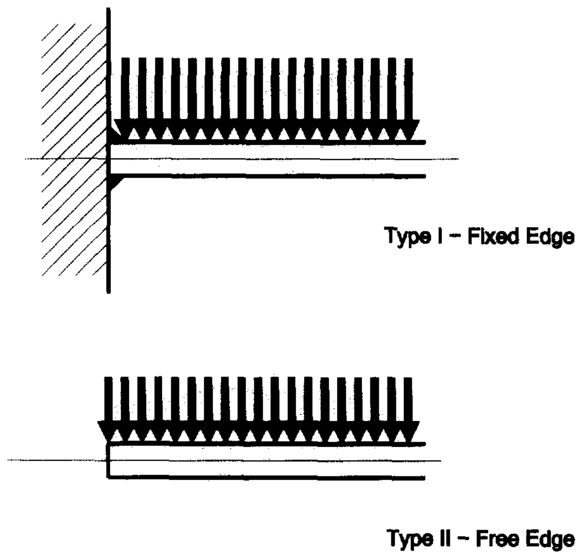

Fig. 3. Possible boundary conditions on the edge of plate.

L, where $L \gg h$. Then, provided the unknowns behave sufficiently well (which does not necessarily have to be the case, especially near a boundary), we can write

$$w \sim L\beta \tag{44}$$

and

$$\frac{\partial}{\partial x} \sim \frac{\partial}{\partial y} \sim \frac{1}{L}. \tag{45}$$

Then, from a dimensional analysis of eqns (33) and (38) in which higher powers of h/L are neglected, we obtain

$$\nabla^2 w + \frac{\partial \beta}{\partial y} = -\frac{q}{2h\eta_L} \tag{46}$$

and

$$\beta + \frac{\partial w}{\partial y} = 0. \tag{47}$$

Equations (46) and (47) are next combined into a single equation in the transverse displacement w of the middle surface, i.e.

$$\frac{\partial^2 w}{\partial x^2} = -\frac{q}{2h\eta_L}. \tag{48}$$

Equation (48) very clearly quantifies what was suggested in Fig. 1. Namely, it suggests that for incompressible and directionally inextensible media subjected to the specific loading case considered herein, the majority of the transverse load is carried by transverse shear. Due to the number of simplifying assumptions made, there are of course some limits to the applicability of eqn (48).

Equation (48) requires only two boundary conditions for the displacement w or for its first derivative, along lines where y is not constant. This means that all of the boundary conditions associated with the full problem cannot be satisfied in the simplified case. None the less, eqn (48) can be used to solve a problem with prescribed displacement w along the boundary (the most common case), albeit with a possible discontinuity along lines of constant y. Evidently, in the neighborhood of such discontinuities, the assumptions in eqns (44) and (45) do not hold; to obtain a meaningful solution, the complete set of eqns (33) and (38) must now be solved.

SAMPLE (NUMERICAL) SOLUTION

The solution of eqns (33) and (38) is by no means trivial. Even assuming simple boundary conditions are imposed, a closed-form solution appears quite difficult to obtain. There are, however, several approximate methods that might be used to solve the problem.

One possibility is a series type of solution. Such solutions were developed by the first author for the analysis of in-plane behavior of inextensible sheets assuming plane stress conditions. Although rather elaborate in nature, these solutions exhibited extremely slow convergence. This is attributed to the presence of "singular lines," a phenomenon described by Rogers (1984) for plane strain analyses, which also applies to plane stress idealizations. Consequently, if series-type solutions are desired, their implementation may require rather elaborate solution schemes. Based upon the above experiences for in-plane behavior, similar difficulties are likely for the solution of the transverse response of inextensible plates.

Furthermore, the high order of differentiation for β present in eqns (33) and (38) renders the search for admissible series expansions impractical.

A second possibility for an approximate solution is the finite element method. However, due to the higher order derivatives of w and β appearing in eqns (33) and (38), the continuity requirements associated with potential elements lessen the feasibility of using this method as a solution technique. One possible remedy to this problem may of course be to use instead the original system of eqns (33)–(36).

In light of the above discussion, eqns (33) and (38) were solved using the finite difference method. To facilitate the solution process, eqn (33) was differentiated with respect to y to obtain

$$\frac{\partial(\nabla^2 w)}{\partial y} = \frac{h^2}{24}\frac{\partial(\nabla^2\beta)}{\partial y^2} - \frac{\partial^2\beta}{\partial y^2} - \frac{1}{2h\eta_L}\frac{\partial q}{\partial y}. \tag{49}$$

Substituting this expression into eqn (38) gives

$$\frac{h^3}{12}(4\eta_T-\eta_L)\frac{\partial^2\beta}{\partial y^2} - \frac{h^5}{360}\eta_L\frac{\partial^2(\nabla^2\beta)}{\partial y^2} + \frac{h^3}{6}\eta_L(\nabla^2\beta) - 2\eta_L\left(\beta+\frac{\partial w}{\partial y}\right) = -\frac{h^2}{12}\frac{\partial q}{\partial y}, \tag{50}$$

which now replaces eqn (38). Approximation of the third derivative of w has thus been avoided. In light of potential complications at the boundary, this is especially desirable. Now the highest order derivative of w appearing in eqns (33) and (50) is the second, and we can live with a single boundary condition on w without resorting to such "tricks" as one-sided difference schemes or "virtual" nodes beyond the boundary.

The sample problem analysed is depicted in Fig. 4. In the analyses performed, the previously discussed (see Fig. 3) boundary conditions for γ_2 were both used, i.e. either $\gamma_2 = 0$ was specified or a condition of $f_{\gamma_2} = 0$ (no transverse traction) was prescribed. The finite difference mesh used consisted of 41×41 nodes. The associated equations were solved iteratively. Some observations pertaining to this solution are noteworthy. Not surprisingly,

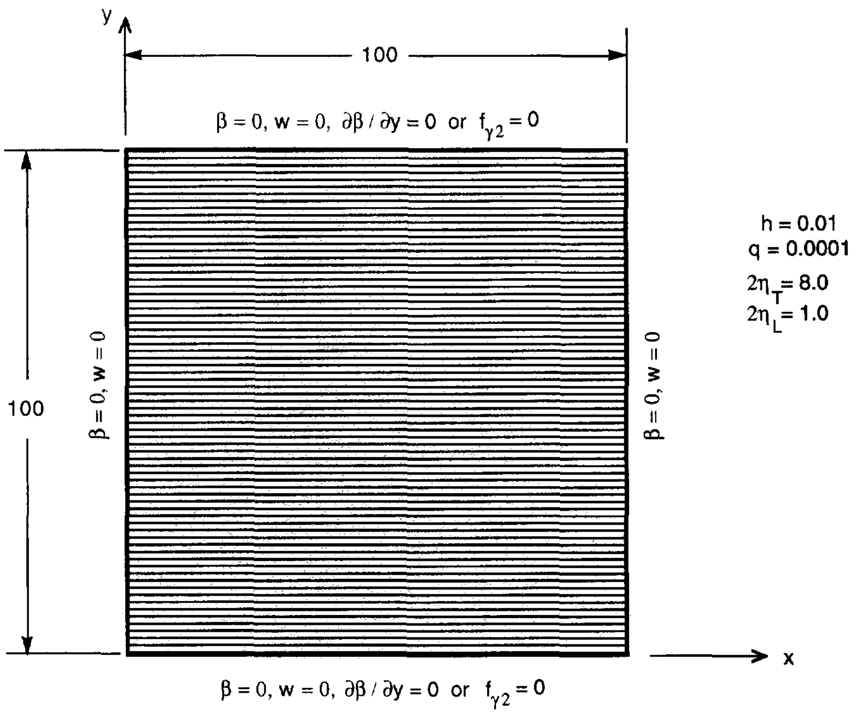

Fig. 4. Schematic illustration of sample fiber-reinforced plate problem.

5

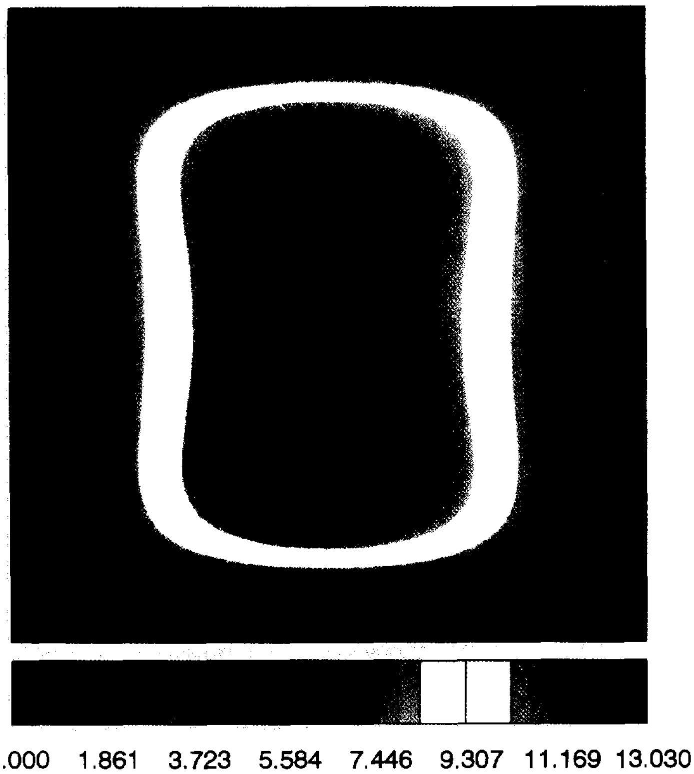

Fig. 5. Transverse displacement w for a plate with opposite edges fixed.

6

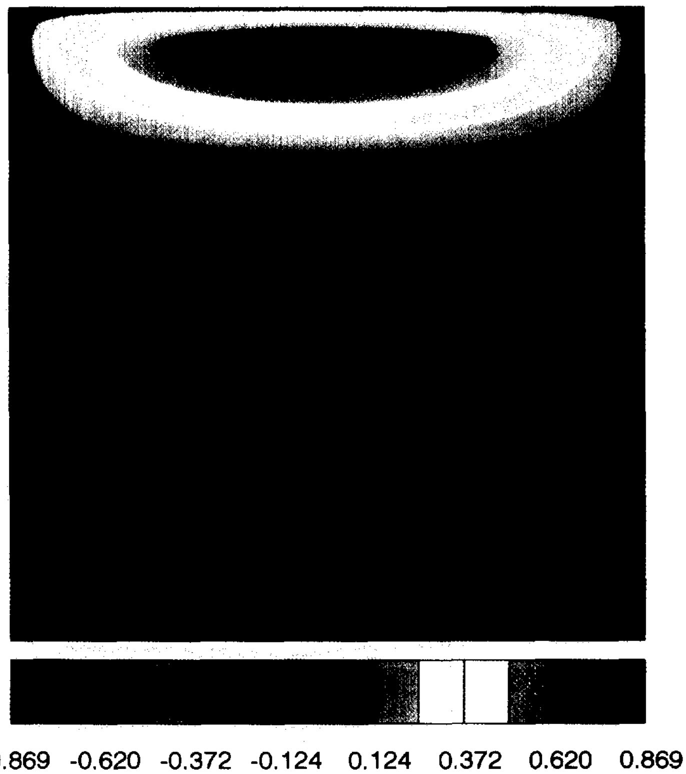

Fig. 6. Rotation β for a plate with opposite edges fixed.

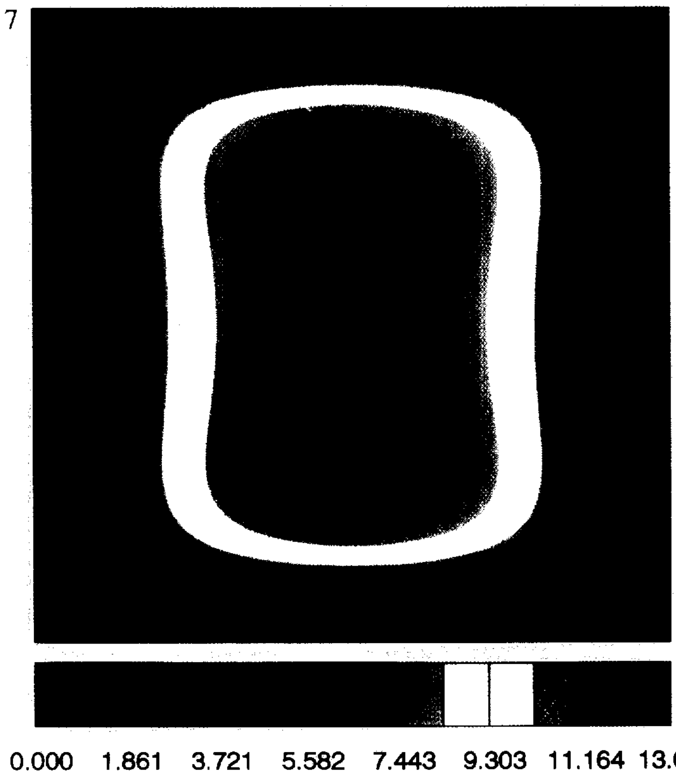

Fig. 7. Transverse displacement w for a plate with zero shear prescribed along opposite edges.

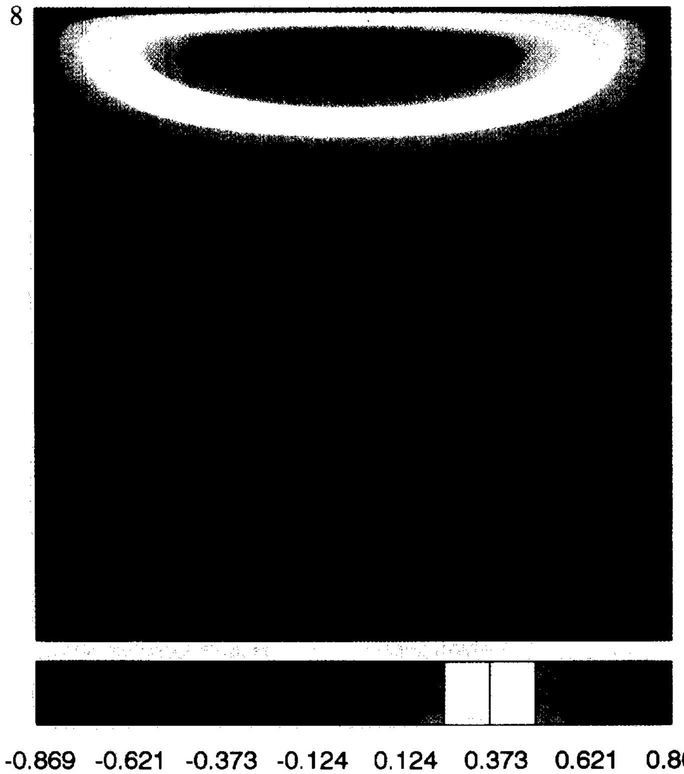

Fig. 8. Rotation β for a plate with zero shear prescribed along opposite edges.

solutions obtained using a standard Gauss–Seidel scheme exhibited rather slow convergence. Although over-relaxation accelerated the convergence, the solution tended to become unstable. As such, for solution of the present problem, the "safer" Gauss–Seidel scheme is recommended. If repetitive solutions for this problem are sought, a more efficient algorithm (e.g. a multi-grid scheme) should be adopted.

The results for w and β associated with the condition that $\gamma_2 = 0$ along two opposite plate edges are shown in Figs 5 and 6; similar results, associated with the boundary condition $f_{\gamma_4} = 0$, are shown in Figs 7 and 8. Evidently there is little difference between the two cases. Given the difficulty of correctly interpreting the boundary condition in question, this is indeed a positive result.

The comparison of the finite difference solution with the simplified solution described, eqn (48), is also rather positive. As is evident from Figs 5–8, in the vicinity of the edges $y = 0$ and $y = 100$, the w and β response exhibits steep gradients; these are necessary in order to simultaneously satisfy both equilibrium and the requirement of a high degree of continuity. This fact, of course, invalidates the assumptions used to derive eqn (48). However, apart from these regions, the comparison of the two solutions proved to be excellent; the maximum deflection of the full solution was very close to the value of 12.5 predicted by eqn (48).

CONCLUSIONS

Based upon certain simplifying kinematic assumptions, the equations governing the response of incompressible plates possessing a direction of inextensibility were derived. The importance of transverse shear, introduced into the discussion based upon rather heuristic arguments, was suitably accounted for in developing the governing equations.

From the form of these equations, it is evident that the restrictions on modeling incompressible inextensible plates are rather severe. Namely, no matter how thin the plate, the standard Kirchhoff assumptions will be invalidated. This has implications for the modeling of extensible plates possessing very high degrees of anisotropy, for it suggests that higher-order thick plate theories should be used.

Similar to other plate theories, the in-plane and transverse response associated with the present formulation uncoupled. The sample analyses performed for the transverse response illustrated two important points. First, away from the boundaries, the extremely simple approximate solution of eqn (48) was found to compare quite favorably with the full solution, thus hinting at the usefulness of the former. Second, the somewhat non-intuitive boundary condition involving γ_2 or the associated applied traction does not seem to significantly influence the solution. As such, the analyst is freed from bothering with this condition, for its proper specification might be hard to formulate.

REFERENCES

Beaussart, A. J. (1990). Numerical modeling of sheet forming processes for thermoplastic composites. Master's Thesis, Department of Mechanical Engineering, University of Delaware.

Coffin, D. W. (1993a). Personal communication.

Coffin, D. W. (1993b). Flange wrinkling and the deep-drawing of thermoplastic composite sheets, Ph.D. Dissertation, Department of Mechanical Engineering, University of Delaware.

Ó Brádaigh, C. M. (1990). Analysis and experiments in diaphragm forming of continuous fiber reinforced thermoplastics. Ph.D. Dissertation, Department of Mechanical Engineering, University of Delaware.

Ó Brádaigh, C. M. and Pipes, R. B. (1992). A finite element formulation for highly anisotropic incompressible solids. *Int. J. Numer. Meth. Engng.* **33**, 1573–1596.

Pipes, R. B., Coffin, D. W., Šimáček, P., Shuler, S. F. and Okine, R. J. (1994). Rheological behavior of collimated fiber thermoplastic composite materials. In *Flow and Rheology in Polymer Composites Manufacturing* (edited by S. G. Advani), Vol. 10, pp. 85–126. Elsevier, Amsterdam.

Rogers, T. G. (1984). Finite deformation and stress in ideal fiber reinforced material. In *Continuum Theory of the Mechanics of Fiber Reinforced Composites* (edited by A. J. M. Spencer), Chapter II, pp. 33–178. Springer, New York.

Rogers, T. G. and Pipkin, A. C. (1971). Small deflections of fiber reinforced beams or slabs. *J. Appl. Mech.* **38**, 1047–1048.

Šimáček, P. (1994). Numerical modeling of sheet forming process. Ph.D. Dissertation, Department of Mechanical Engineering, University of Delaware.

Šimáček, P., Kaliakin, V. N. and Pipes, R. B. (1993). Pathologies associated with the numerical analysis of hyper-anisotropic materials. *Int. J. Numer. Meth. Engng* **36**, 487–3508.

Spencer, A. J. M. (1984). Constitutive Theory for Strongly Anisotropic Solid. In *Continuum Theory of the Mechanics of Fiber Reinforced Composites* (edited by A. J. M. Spencer), Chapter I, pp. 1–32. Springer, New York.